Journal of Physics: Conference Series

Fabrication of 2D and 3D Electromagnetic Metamaterials for the Terahertz Range.

To cite this article: B D F Casse *et al* 2006 *J. Phys.: Conf. Ser.* **34** 885

Institute of Physics Publishing Journal of Physics: Conference Series **34** (2006) 885–890
doi:10.1088/1742-6596/34/1/147 International MEMS Conference 2006

Fabrication of 2D and 3D Electromagnetic Metamaterials for the Terahertz Range.

B. D. F. Casse[1], H. O. Moser[1†], L. K. Jian[1], M. Bahou[1], O. Wilhelmi[2], B. T. Saw[1] and P. D. Gu[1]

[1] Singapore Synchrotron Light Source, National University of Singapore, 5 Research Link, Singapore 117603

[2] now at: FEI Electron Optics BV, Achtseweg Noord 5, 5621 GG Eindhoven, The Netherlands

E-mail: †moser@nus.edu.sg

Abstract. This paper addresses the 2D and 3D micro- and nanofabrication of ElectroMagnetic MetaMaterials (EM^3) for the terahertz range. EM^3 refers to artificial composite materials which consist of a collection of repeated metal elements designed to have a strong response to applied electromagnetic fields, so that near resonance both the effective permittivity ϵ and magnetic permeability μ become simultaneously negative. This unusual situation leads to exotic consequences such as a negative index of refraction and an inverse Doppler and Čerenkov effect. EM^3 fabricated so far have been mostly two-dimensional and in this respect are highly anisotropic. By anisotropic, it is inferred that the response of the system depends on the direction of illumination. The anisotropic nature of the metamaterials impedes eventual real-life applications of the negative media as it places constraints on the impinging electromagnetic waves. Ways of producing three-dimensional (3D) or more isotropic EM^3 by means of tilted x-ray exposures will be introduced. Basic geometry tells us that if the structures are inclined at 30–45°, this would lead to an improvement of the coupling of the $\overline{H}$ vector by 50–70%.

1. Introduction

The response of materials to electromagnetic radiation is characterized by Maxwell's equations and the constitutive relations involving the permittivity ϵ and permeability μ. Nearly all familiar materials have positive values for both ϵ and μ. But it is not unusual for some materials to have a negative permittivity, e.g., metals from zero frequency to the plasma frequency. However, a negative permeability at optical frequencies does not occur in natural materials. In 1967, V. G. Veselago theoretically investigated materials with simultaneously negative permittivity ϵ and permeability μ [1]. He coined the word "*left-handed materials*" (LHM) for such media due to the left-handed triad formed by the vectors $\overline{E}$, $\overline{H}$ and $\overline{k}$. Veselago predicted that such a medium would exhibit exotic properties such as a negative index of refraction and an inverse Doppler and Čerenkov effect. His analysis of materials with negative parameters has remained a curious exercise in electromagnetic theory for a span of thirty years simply because materials with both negative permittivity and permeability could not be readily found in nature. However, in the 1990s, Pendry and co-workers began looking into theoretical models of how to artificially engineer electromagnetic metamaterials— Pendry showed that a combination of metallic wires [2] and Split Ring Resonators (SRRs) [3] could lead to $\epsilon_{\text{eff}} < 0$ and $\mu_{\text{eff}} < 0$ respectively. The metamaterial envisioned by Pendry is a collection of repeated elements designed to have a strong response to applied electromagnetic fields. This led to a resurgence of effort in developing structures with novel materials properties, with first demonstrations in the GHz range [4] or the microwave region. To fabricate such artificial materials, the size and spacing of the elements should be much smaller than the electromagnetic wavelengths of interest so that incident radiation cannot distinguish the collection of elements from a homogeneous material. If we want metamaterials operating at the infrared region or even at optical frequencies, then the overall structure sizes of the individual components have to be shrunk to the order of µm and nm respectively. Since 2003, we applied lithography to the manufacturing of the next generation EM^3, succeeding in producing the first microelectromagnetic metamaterials at the far infrared region [5]. Continuing these efforts towards nanofabrication[6] [7], we were able to produce electromagnetic metamaterials operating at a record frequency of ∼187 THz [8].

We present micro- and nanofabricated rod-split-ring resonators (RSRs) with overall structure size below 100 µm (structural details down to 5 µm) and 1 µm (structural details down to 50 nm) respectively. The resonance frequencies of the RSRs are in the spectral range 1–187 THz. Finally we address the issue of producing more isotropic or 3D EM^3 via tilted exposures during X-ray lithography.

2. Analysis of the planar design for micro/nanofabrication

For rapid prototyping of metamaterials, a planar adaptation of the Pendry-Smith's model [4] was used, with rods and SRR in the same plane as shown in figure 1.

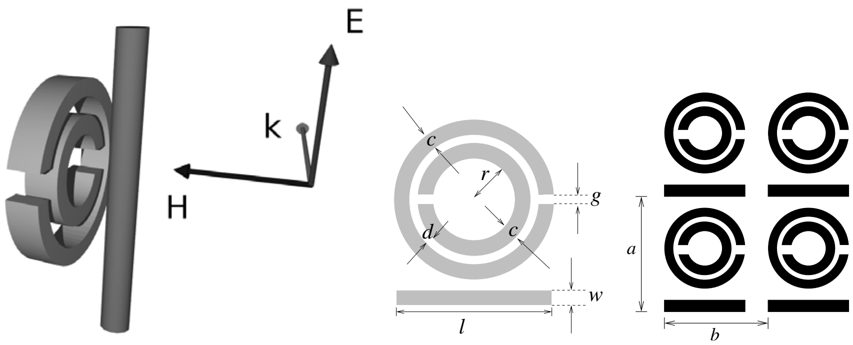

(a) (b)

Figure 1: (a) The Pendry-Smith model metamaterial unit cell. (The arrows denote the direction of the wave vector $\overline{k}$, the electric field component $\overline{E}$, which is along the direction of the wire medium, and the magnetic component $\overline{H}$, which is parallel to the axis of the SRR.) (b) The planar adaptation of Pendry-Smith prototype for 2D micro/nanofabrication. Geometric parameter definition shown as well as the periodic arrangement of unit cells.

Recent numerical simulations [9] confirm that both models can lead to the realization of negative parameters materials.

In the Pendry model, the rods have a negative permittivity just below their plasma frequencies, ω_p as described by the Drude model [10]. The mechanism proposed by Pendry [2] to lower the plasma frequencies is to build thin wires and thereby diluting the average concentration of electrons and enhancing the effective electron mass through self-inductance. The overall effect lowers the plasma frequency. The split ring resonator (SRR) can be viewed as an LC circuit [3]: A time-varying magnetic field applied parallel to the axis of the rings induces an emf in the plane of the element, driving currents within the 'split rings' which result in a dispersive effective permeability.

While the usable bandwidth for which $\epsilon_{\text{eff}} < 0$ is much larger than that of $\mu_{\text{eff}} < 0$, provided that a small ratio of radius to distance of the wires is used, the lower and upper limit of the frequency interval over which $\mu_{\text{eff}} < 0$ was calculated from Pendry's analytical formula [3]

$$\nu_0 = \frac{1}{2\pi}\sqrt{\frac{3dc_0^2}{\pi^2 r^3}} < \nu_{\text{mp}} = \frac{\nu_0}{\sqrt{1-\pi r^2/ab}} \tag{1}$$

where c_0 is the speed of light *in vacuo*. Five and four geometric variants were used for the micro- and nanofabrication of EM^3, respectively. The sets of those geometric parameters and the limits of the interval in which the composites have EM^3 behavior are shown in tables 1 and 2.

Table 1: THz specifications of a Rod-Split-Ring structure for microfabrication.

	r/μm	c/μm	d/μm	a/μm	b/μm	ν_0/THz	ν_{mp}/THz
Ni Slim	10	10	10	110	90	2.63	2.68
Ni Fat	10	15	10	135	110	2.63	2.67
Au 1	8.4	12	4.3	95.4	78.4	2.24	2.28
Au 2	11	12	4.3	100.6	83.6	1.50	1.53
Au 3	14	12	4.3	106.6	89.6	1.04	1.08

For all structures $g = 5$ μm, $l = (r + 2c + d) \times 2$. For Ni, $w = 10$ μm while for Au, $w = 12$ μm.

Table 2: THz specifications of a Rod-Split-Ring structure for nanofabrication.

Samples	r/nm	c/nm	d/nm	a/µm	b/µm	ν_0/THz	ν_{mp}/THz
S1	300	200	100	2.00	1.70	50.66	52.91
S2	150	90	80	1.07	0.90	128.16	133.14
S3	120	90	80	1.01	0.84	179.11	184.09
S4	90	90	40	0.79	0.66	194.99	199.93

For all structures $g = 50$ nm, $w = c$, $l = (r + 2c + d) \times 2$

3. Micro/nanofabrication and characterization of 2D electromagnetic metamaterials

For the microfabrication process, the structures were produced in a plastic matrix (AZ P4620 photoresist) by first laser beam direct writing, then development thereby creating voids, and subsequently filling voids with metal by electroforming. The metal structures embedded in the matrix are finally released from the silicon substrate by etching the chromium sacrificial layer in between resist and substrate. The final products are 2 × 2 mm^2 microchips consisting of nickel or gold RSRs held in the AZ P4620 plastic matrix as shown in figure 2 (a). Details of the microtechnology process are outlined in reference [5].

The nanofabrication process starts with electron beam writing into PMMA resist sitting on top of either a glass or a silicon substrate. In this case, the substrate is transparent within the relevant spectral range and therefore release of the metal-filled matrix is not necessary. The voids created by the development are then filled with metal via magnetron sputtering. A final lift-off of the PMMA resist was achieved by immersing the sample in acetone for 1 hour. The end product is 500 × 500 µm^2 of 30 nm thick gold RSR on 0.5-mm thick glass substrate as shown in figure 2 (b). A detailed account of the nanofabrication processes is found in references [6]–[8].

The spectroscopic measurements (in transmission mode) were performed using a Bruker IFS 66 v/S Fourier transform interferometer, at the Infrared Spectro-MIcroscopy beamline (ISMI), in the far infrared (FIR) over the range of 22 to 400 cm^{-1} with a 4 cm^{-1} and 2 cm^{-1} spectral resolution. The microchips were mounted in the FTIR at normal incidence to the unpolarized beam. Axial magnetic field components needed to induce the current in the split rings are due to misalignment of the sample with respect to the beam and diffraction at the surface.

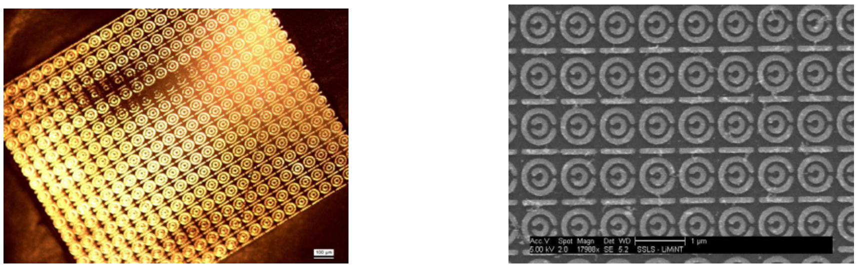

(a) (b)

Figure 2: (a) 2 × 2 mm^2 gold RSRs microchips embedded in the AZ P4620 plastic matrix (scale bar 100 µm). (b) 500 × 500 µm^2 of 30 nm thick gold RSRs on 0.5-mm thick free-standing glass substrate (scale bar 1 µm).

As expected the RSR samples showed characteristics of a bandpass filter in the relevant spectral region as shown in figure 3 (a).

Transmission experiments on the nanoEM^3 composites were performed with Bruker's Hyperion 2000 Microscope at the ISMI beamline. The Hyperion microscope was set to reflection-transmission mode for the experiment, meaning transmission through the sample, followed by a reflection on a silver mirror and a second transmission through the sample before reaching the detector. The incident angle of the beam on the samples was 23° to the normal, as set by the Schwarzschild objective. Again the samples exhibited prominent upward-pointing transmission peaks as shown in figure 3 (b).

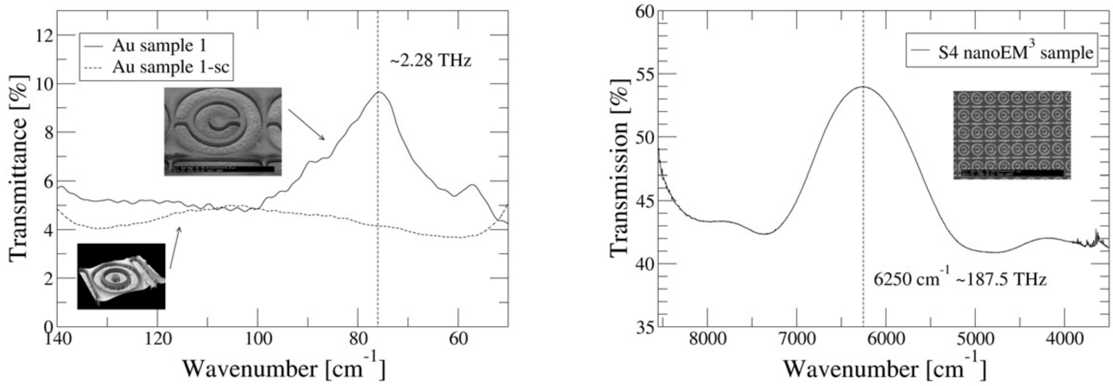

(a) (b)

Figure 3: (a) Measured transmission curve of microfabricated gold RSRs sample 1 and short-circuited (-sc) SRRs (i.e. SRR with the azimuthal gap g closed). The RSR sample exhibit EM^3 behavior in the FIR at $\sim$ 2.3 THz while the short-circuited SRRs do not show any prominent spectral response. (b) Measured transmission curve of nanofabricated Sample S4. Resonance occurs near telecommunications frequencies (193 THz $\simeq$ 1.55 µm)

Figure 4 shows the plot of inner radius versus frequency for split ring resonators over the spectral range from 1 THz to 1 PHz. Symbols mark measured results and $\nu_0(r)$ is the logarithm of Pendry's analytical formula introduced in equation (1). The experimental results are in good agreement with both Pendry's analytical formula and numerical simulations (not shown in this paper).

4. Fabrication concepts of 3D electromagnetic metamaterials

Metamaterials produced so far in the terahertz range have been more or less flat metal structures or 2D and in this respect are highly anisotropic. By anisotropic it is inferred that the response

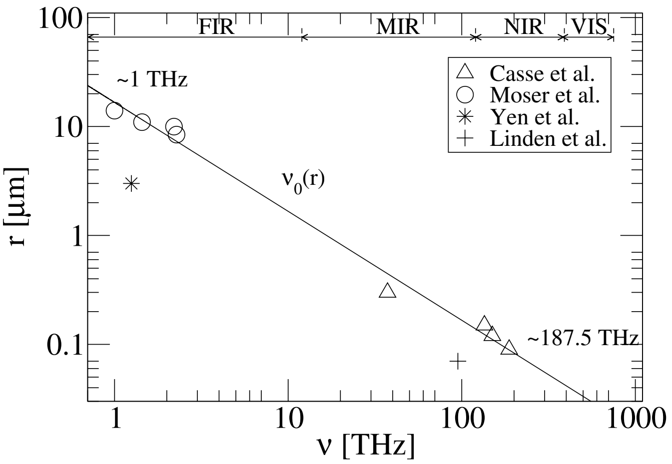

Figure 4: Plot of radius r of the SRR versus frequency over the spectral range from 1 THz to 1 PHz. The open symbols mark measured results while the symbols (∗) and (+) denote results obtained by Yen *et al.* [11] and Linden *et al.* [12], respectively. The straight line is Pendry's formula for the resonance frequency of a circular nested SRR.

of the system depends on the direction of illumination. For example, the split ring resonators respond to a magnetic field that is polarized parallel to their axis while the rods respond to an electric field polarized along their lengthwise direction. Gay-Balmaz and Martin [13] were among the first to propose more 3D EM^3 by assembling flat EM^3 structures such that they offer full coupling for the incident electric and magnetic fields in two or three orthogonal directions. Although the model they proposed is commendable, it becomes highly impractical to assemble planar unit cells when it comes to micron-size structures and below.

SSLS is working on the production of more isotropic 3D structures within the same matrix. In lithography, it is usual to expose the mask-substrate stack perpendicularly. It is however possible to vary the angle of incidence to obtain inclined exposures as shown in figure 5 (a). The stack could even be rotated either continuously or to different positions between exposures. This tilting, rotating and even wobbling was proposed several years ago [14] [15]. These techniques are revived to produce EM^3 structures in which the axes of the SRRs would cover two (or even three) intersecting or perpendicular directions so that the incident field can always couple efficiently to the SRRs as shown in figure 5 (b).

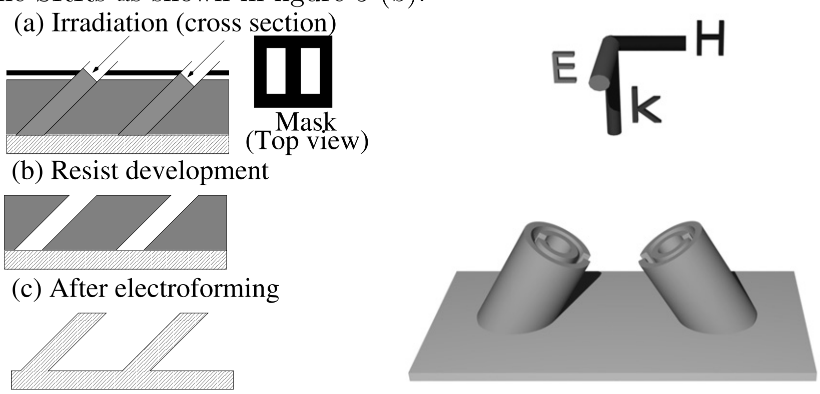

(a) (b)

Figure 5: (a) Principle of making inclined exposures in X-ray lithography. (b) 3D inclined SRR structures within the same matrix. Inclination of 30–45° will lead to an improvement of the coupling of the $\overline{H}$ vector by 50–70%.

In structures inclined at 30–45°, this leads to an improvement of the coupling of the $\overline{H}$ vector by 50–70%.

5. Conclusion

We have produced 2D composite materials, so-called Rod split Ring Resonators (or RSRs), by lithography-based micro- or nanofabrication. The microfabricated RSRs possessed an outer ring diameter in sub 100 µm (and structural details down to 5 µm) while the nanofabricated RSRs had an outer ring diameter of ∼1 µm (and structural details down to 50 nm). Analytical and numerical simulations confirm that the RSR exhibit EM^3 behavior between 1 (far infrared region) and 187 THz (near infrared) which is close to telecommunications frequencies (193 THz $\simeq$ 1.55 µm). Work is underway to use tilted X-ray exposure schemes to produce more 3D EM^3 so as to reduce anisotropy and increase the practicality of the latter in future applications.

Acknowledgments

The authors would like to thank Prof. Lim Hock and Mr. Gan Yeow Beng from the Temasek Laboratories, NUS, for valuable discussions. This work was performed at the Singapore Synchrotron Light Source (SSLS) under A*STAR/MOE RP3979908M, A*STAR 0121050038, and NUS Core Support C-380-003-003-001 grants.

References

[1] V. G. Veselago. *Sov. Phys. Usp.*, 10:509, 1968.

[2] J. B. Pendry, A. J. Holden, W. J. Stewart, and I. Youngs. *Phys. Rev. Lett.*, 76:4773, 1996.

[3] J. B. Pendry, A. J. Holden, D. J. Robbins, and W. J. Stewart. *IEEE Trans. Microwave Theory Tech.*, 47:2075, 1999.

[4] D. R. Smith, Willie J. Padilla, D. C. Vier, S. C. Nemat-Nasser, and S. Schultz. *Phys. Rev. Lett.*, 84:4184, 2000.

[5] H. O. Moser, B. D. F. Casse, O. Wilhelmi, and B. T. Saw. *Phys. Rev. Lett.*, 94(6):063901, 2005.

[6] B. D. F. Casse, H. O. Moser, O. Wilhelmi, and B. T. Saw. *Micro- and Nano-Fabrication of Electromagnetic Metamaterials for the Terahertz range.* pages 18–25, Singapore, 2005. World Scientific.

[7] H. O. Moser, B. D. F. Casse, O. Wilhelmi, and B. T. Saw. *Electromagnetic Metamaterials over the whole THz range — achievements and perspectives.* pages 55–58, Singapore, 2005. World Scientific.

[8] B. D. F. Casse, H. O. Moser, M. Bahou, L. K. Jian, and P. D. Gu. *in press for IEEE Transactions on Nanotechnology*, 2006.

[9] M. Kafesaki, Th. Koschny, R. S. Penciu, T. F. Gundogdu, E. N. Economou, and C. M. Soukoulis. *J. Opt. A: Pure Appl. Opt.*, 7:S12–S22, 2005.

[10] D. Pines and D. Bohm. *Phys. Rev.*, 85:338, 1952.

[11] T. J. Yen, W. J. Padilla, N. Fang, D. C. Vier, D. R. Smith, J. B. Pendry, D. N. Basov, and X. Zhang. *Science*, 303:1494, 2004.

[12] Stefan Linden, Christian Enkrich, Martin Wegener, Jianfeng Zhou, Thomas Koschny, and Costas M. Soukoulis. *Science*, 306:1351, 2004.

[13] P. Gay-Balmaz and O. J. F. Martin. *J. Appl. Phys.*, 81(5):939–941, 2002.

[14] H. O. Moser, W. Ehrfeld, M. Lacher, and H. Lehr. *Fabrication of Three-dimensional Microdevices from Metals, Plastics and Ceramics.* Besançon, France, October 20–22 1992. Institut des Microtechniques de Franche-Compté.

[15] W. Bacher, P. Bley, and H. O. Moser. *Optoelectronics Interconnects and Packaging, SPIE Critical Reviews of Optical Science and Technology*, CR62:442–460, 1996.